NANO LETTERS

LETTER

pubs.acs.org/NanoLett

Nonlinear Optical Processes in Optically Trapped InP Nanowires

Fan Wang,[†] Peter J. Reece,[*,†] Suriati Paiman,[‡,§] Qiang Gao,[‡] Hark Hoe Tan,[‡] and Chennupati Jagadish[‡]

[†]School of Physics, The University of New South Wales, Sydney, NSW 2052, Australia

[‡]Research School of Physics and Engineering, The Australian National University, Canberra, ACT 0200, Australia

[§]Department of Physics, Faculty of Science, Universiti Putra Malaysia, 43400 Serdang, Selangor, Malaysia

ABSTRACT: We report on the observation of nonlinear optical excitation and related photoluminescence from single InP semiconductor nanowires held in suspension using a gradient force optical tweezers. Photoexcitation of free carriers is achieved through absorption of infrared (1.17 eV) photons from the trapping source via a combination of two- and three-photon processes. This was confirmed by power-dependent photoluminescence measurements. Marked differences in spectral features are noted between nonlinear optical excitation and direct excitation and are related to band-filling effects. Direct observation of second harmonic generation in trapped InP nanowires confirms the presence of nonlinear optical processes.

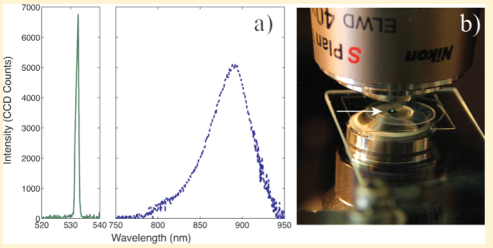

KEYWORDS: semiconductor nanowires, photoluminescence, optical tweezers, multi-photon absorption, second harmonic generation

Geometrically regular semiconductor nanowires are of considerable interest for nanoscale optoelectronic integrated circuits and devices. With cross-sectional dimensions of the order of tens to hundreds of nanometers and lengths extending up to tens of micrometers, nanowires can potentially function as both electrical[1] and optical[2] conduits. Importantly, semiconductor nanowires offer a high level of control over the composition, enabling the incorporation of functional elements such as quantum heterostructures[3] and heterojunctions,[4] radially and along the axis of the nanowire. Multiple interconnecting nanowires provide all the elements to create a fully functional microprocessor.[5]

Nanowires based on InP offer the same advantages afforded by their bulk counterpart in terms of photonic circuits, but with the possibility of higher density integration and greater flexibility for direct assembly on low-cost substrates.[6] The structural properties of InP nanowires are distinct from bulk InP as they support the formation of a hexagonal wurtzite (WZ) crystal phase, which has an increased band gap energy, compared to the normal zinc blende (ZB) phase.[7] The combination of these two phases leads to type II band offset homojunctions with shallow barrier heights of 45 meV for the conduction band and 124 meV for the valence band. InP nanowires exhibit strong room temperature luminescence by virtue of low surface recombination velocity, and the characteristic emission has signatures from both poly type crystalline phases. A broader emission band compared with bulk InP can be traced to free carrier recombination dynamics across the type II homojunction.[8]

Multiphoton absorption processes enable optical excitation in semiconductors where the absorbed photon energy is below the energy of the band gap; thermalization of the free carriers to the band edge and subsequent radiative recombination yield photoluminescence at a wavelength corresponding to the band gap energy. The general form for the rate of multiphoton absorption in semiconductors for a given incident intensity I is given by $K_N I^N$, where N is the number of absorbed photons and K_N is the N-photon absorption coefficient.[9] The magnitude of multiabsorption coefficients strongly depends on the material of interest and is, in general, not well quantified experimentally for processes involving three or high numbers of photons. Other nonlinear processes, such as second and third harmonic generation, may also be possible and produce photons with energies above the band gap of the material and also band-edge luminescence through reabsorption of the high-energy photons.

In this Letter we present our findings on the effect of two photon absorption (TPA) related photoluminescence, as well as second (SHG) and third harmonic generation (THG) processes in InP nanowires that are trapped in a gradient force optical tweezers. The light emitting properties are compared to luminescence via direct excitation for both crystal polytypes and referenced against bulk InP samples. Strong spectral blueshifts are observed between nonlinear and direct optical excitation related emission, which we associate with band filling effects. The magnitudes of the shifts are discussed in the context of the presence of type II homojunctions present in InP nanowires. Power-dependent photoluminescence reveals both quadratic and cubic dependence indicating both two photon and three photon processes are occurring. Direct observation of SHG in InP nanowires confirms the presence of sum frequency generation.

Figure 1 gradient force optical tweezers incorporating microphotoluminescence spectroscopy.[10] In this arrangement a linearly polarized 1064 nm YAG laser (5 W Laser Quantum, 1064 Ventus) is directed to the back aperture of a high numerical aperture (NA = 1.25) oil immersion objective (Nikon E-plan 100×), via relay optics, in order to create a diffraction limited

Received: June 16, 2011
Revised: August 15, 2011
Published: August 29, 2011

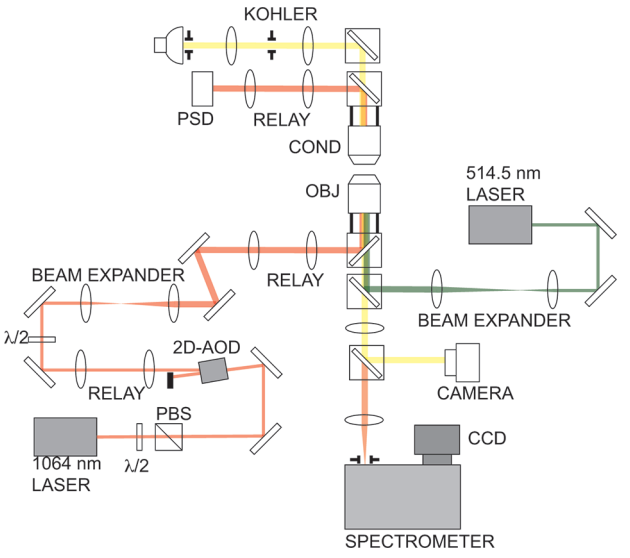

Figure 1. Experimental setup used for studying nonlinear optical processes in optically trapped nanowires. The optical tweezers arrangement consists of a 1064 nm laser source, external power control, acousto-optic beam steering, and a high NA focusing objective. An argon laser collinearly aligned is used to directly excite nanowire samples. Bright field microscopy is used to visualize the optically trapped nanowires, and a position sensitive diode is used to track their motion. Spectra are recorded using a grating spectrometer and CCD array.

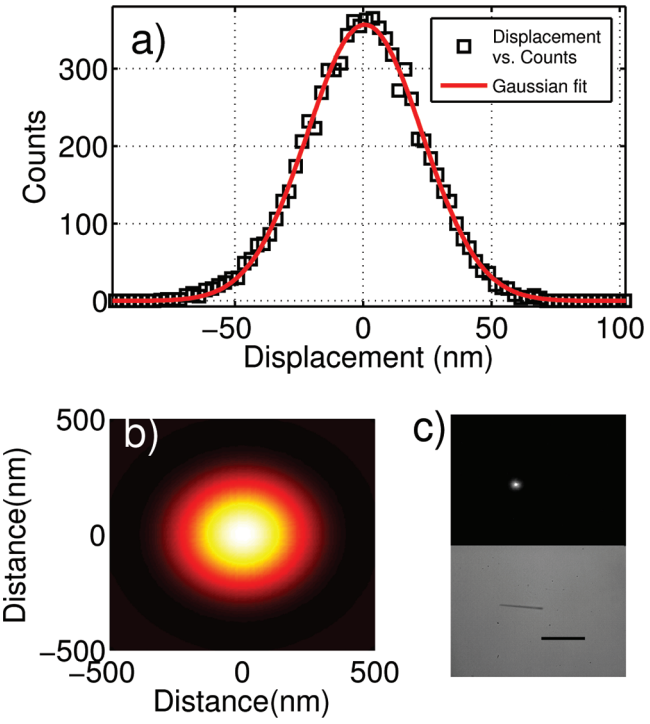

Figure 2. (a) The histogram and corresponding Gaussian fit of the motion of the trapped nanowire relative to the trapping center for a trapping intensity of 30 mW. (b) Simulated beam profile of the optical trapping beam at the microscope objective focus. (c) The top panel is an image of luminescence from optically trapped nanowire; the nanowire is aligned with the long axis orthoganol to the field of view. The bottom panel shows a bright field image of a free-floating nanowire with the long axis clearly visible. The black bar indicates 10 μm.

spot in the front focal plane. A two-axis acousto-optic deflector (AOD) (NEOS Technologies) provides automated control of the position of the laser within the objective field of view. A half waveplate and polarizing beam splitter are used to control the power of the beam, and a second waveplate is used to control the polarization in the focal plane. The absolute power at the focus is measured using a calibrated photodetector (Coherent Fieldmaster) taking into account the transmission losses of the optical system and microscope objective. A 514.5 nm argon ion laser (Coherent Innova 70) aligned collinearly with the trapping laser is used for direct photoexcitation of the nanowires; photoluminescence is collected using a grating spectrometer and recorded using a charge coupled device (CCD) (Princeton Instruments, PIXIS). Imaging of optically trapped nanowires is done with a bright field condenser and fast CCD camera (Basler); Brownian dynamics of the nanowires was recorded with a position sensitive detector (Silicon Pacific Sensors), using back focal-plane interferometery.

InP nanowires are epitaxially grown on InP (111)B substrates by metal−organic chemical vapor deposition (MOCVD). The semiconductor substrates are initially immersed in poly-L-lysine solution and treated with gold colloid solution. The nanowires are then grown in the MOCVD reactor using trimethylindium and phosphine (PH_3) precursors, with 30 nm gold nanoparticles acting as seeds for growth via the vapor−liquid−solid (VLS) mechanism. During growth, pressure was kept at 100 mbar while the temperature was set at 490 °C, with a V/III ratio of 44, and the growth time is approximately 20 min.[11] All nanowires were transferred from the native substrate to an aqueous solution by sonication, leading to a dispersion of nanowires with lengths varying from 5 to 15 μm. A nanowire immobilized on the surface of a coverslip is shown in the lower panel of Figure 2c.

In the optical tweezers arrangement described above, InP nanowires are stably trapped with their long axis aligned to the propagation direction of the beam.[10] This trend follows that of other types of semiconductor nanowires in a similar arrangement.[12] The trapped nanowires experience fluctuations in their position due to stochastic motion, viscous damping, and the optical restoring force. This motion may be quantitatively investigated using back focal plane interferometery.[13] Figure 2a shows a histogram of the position fluctuations of the nanowire when the trapping power is set to 30mW in the focal plane. In this instance, the nanowire position is confined to a region of ±30 nm around the focus, which is considerably smaller than the beam spot size, which was estimated to be 600 nm from multiple multipole expansion calculations (Figure 2b).[14] With these parameters the intensity of the 1064 nm laser incident on the nanowires was estimated to be 13.7 MW/cm^2. As the trapping power is increased, the trap stiffness is increased and the nanowires become more confined to the center of the beam—this indicates that Brownian dynamics has a minimal effect on the excitation intensity experienced by the nanowires.

Figure 3 shows the normalized photoluminescence from optically trapped nanowires where excitation is achieved by nonlinear excitation with the trapping source (dotted) and direct excitation with the argon laser (solid). For the nanowires we present photoluminescence from nanowires with predominantly WZ (Figure 3a) and ZB (Figure 3b) crystal phases. Also presented is luminescence from a bulk InP sample (Figure 3c). It should be noted that both WZ and ZB nanowires in InP are not pure crystal phases as spontaneous formation of twinning defects is always present and leads to the presence of regions of the other

dx.doi.org/10.1021/nl2020262 |*Nano Lett.* 2011, 11, 4149–4153

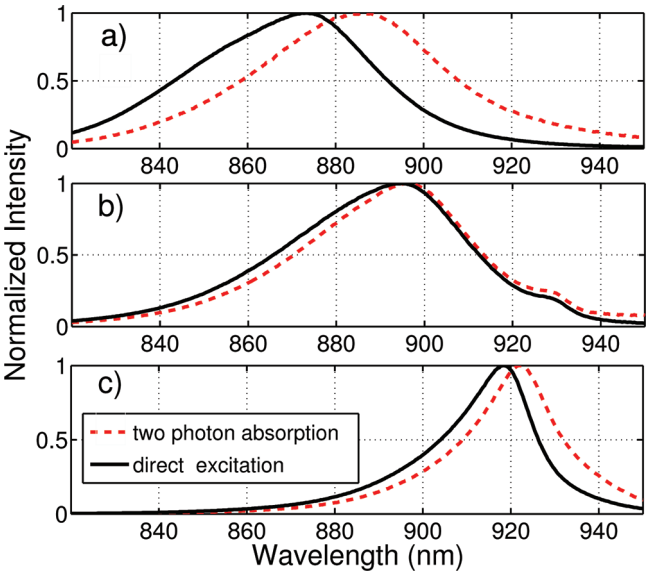

Figure 3. Photoluminescence spectra resulting from for two photon absorption (dotted) and direct excitation (solid) for (a) a wurtzite (WZ) phase nanowire, (b) a zinc blende nanowire, and (c) bulk InP substrate.

crystal polytype. However, through optimization of the growth conditions it is possible to achieve predominately one crystal phase.[11] The intensity of the trapping laser under nonlinear photoexcitation related emission is 154 mW (70.7 MW/cm^2), while the incident power of the argon laser under direct excitation was 157 μW (0.236 MW/cm^2). As the photon energy of the trapping laser is significantly below the band gap energy of InP, we do not expect direct promotion of free carriers to the conduction band and thus ascribe the observed luminescence to nonlinear photoexcitation, such as two photon absorption (TPA). The spectra presented in the Figure 3 have been normalized, but the nonlinear photoexcitation related emission per milliwatt of excitation power is observed to be typically 1000 times weaker than the directly excited photoluminescence; this is consistent with an expected weaker emission intensity from multiphoton absorption processes. For the WZ phase nanowires, we observe a marked blue-shift (13 nm) in the emission peak position for direct excitation and a broadening of the peak at the short wavelength edge. Under similar excitation conditions predominantly ZB nanowires (<1 nm) and bulk InP (4 nm) exhibit a measurable but less pronounced blue shift.

We may understand the peak shift in terms of the Burstein−Moss effect which predicts a shift in the emission spectrum as the low lying states in the conduction band are populated by free carriers under strong photoexcitation.[15] Under nonlinear photoexcitation the free electrons populating the conduction band are considered to be very small; under direct excitations, states at the bottom of the conduction band are filled by a large number of photoexcited carriers and the radiative recombination occurs between the highest filled energy level. In bulk direct band gap semiconductors, the density of states near the band edge is proportional to square root of the energy above the band gap.[16] In Figure 4b we show the peak shift of the nonlinear photoexcitation related luminescence as a function of trapping intensity. In the ZB nanowires we note that the peak shift is very small and is stable with increasing nonlinear excitation. At very high excitation energies the peak shift tends

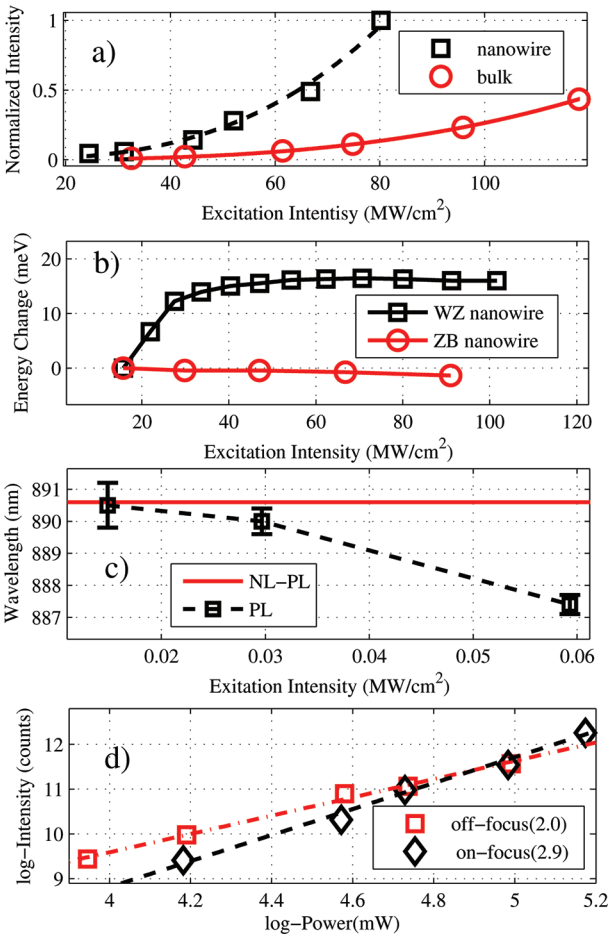

Figure 4. (a) Peak photoluminescence intensity as a function of incident power of the infrared trapping laser for single nanowire (squares) and bulk (circle) InP; the dotted lines indicate a cubic fit to the data. (b) Energy increase in the band-edge emission as a function of trapping power for the ZB InP samples (circles) and WZ InP nanowires (squares). (c) Peak wavelength WZ nanowire photoluminescence as a function of direct excitation internsity; the solid red line indicates the position of the peak wavelength for nonlinear photoexcitation. (d) log−log plot of nonlinear optical excitation related photoluminescence intensity versus trapping power at two different positions along the axis of a ZB nanowire: at the trapping focus (diamond) and away from the focus (squares) (measurements performed on different nanowires). The gradient of the curves (shown in brackets) indicates a corresponding cubic and quadratic dependence.

to red-shift and we associate this with the onset of heating which causes a reduction in the band gap. In the case of the WZ nanowires, emission energy initially blue-shifts strongly with increasing trapping power and is followed by a much smaller shift at higher intensities. We may expect the comparatively large peak shift is related to initial filling of a relatively small number of low energy states introduced by the twinning defects.[17] This is in contrast to the expect shift which should follow a 4/3 power dependence.[16] At very high excitation intensities we again see a small red-shift in the peak position which we associate with heating. Further evidence for band-filling is shown in Figure 4c, where we reduce the direct excitation intensity and observe that the photoluminescence peak red-shifts toward the position of the nonlinear excitation.

dx.doi.org/10.1021/nl2020262 |*Nano Lett.* 2011, 11, 4149–4153

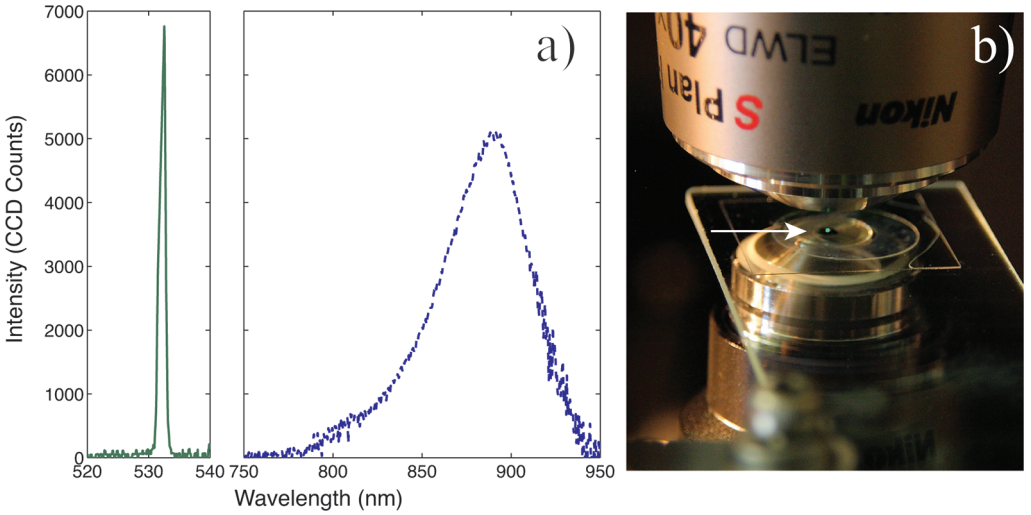

Figure 5. (a) Emission spectrum from a single optically trapped nanowire showing both second harmonic generation and band-edge emission. The trapping power at the focus is 200mW. (b) Green light emission is directly observable at the focus of the objective with the naked eye—indicated here by the arrow.

Figure 4a shows the power dependence of the peak intensity with infrared trapping power; this provides further evidence for the origin of the nonlinear photoexcitation. The emission in this instance follows a clear cubic dependence; a similar trend is also observed in the bulk InP samples. As the power dependence of two photon absorption is expected to be quadratic, this implies that other types of nonlinear processes are likely to dominate in the intensity range that we are working with. We also note from Figure 4a that the InP nanowire provides stronger emission than the bulk sample. While a direct quantitative comparison is difficult as excitation conditions differ between the two cases, an enhancement from nanowires might be expected due to improved light extraction efficiency at the emission wavelength.

We propose two possible mechanisms for the observation of the cubic power dependence of the luminescence at the focus of the trapping laser: (i) three photon absorption or (ii) third harmonic generation (THG) followed by reabsorption. We may discount three photon absorption as a likely candidate by considering the scaling behavior of multiphoton absorption proposed by Brandi and de Araujo.[18] This work suggest that the incident beam intensity for which two and three photon absorption is comparable should be approximately 250 GW/cm^2 for InP, which is several orders of magnitude higher than typical intensities (50 MW/cm^2) used in this study. This also suggests that two-photon absorption should be the dominant mechanism for photon absorption below the band gap energy under the excitation conditions presented. THG is also possible in InP samples, as this material has a non-negligible $\chi^{(3)}$ nonlinear susceptibility.[19] Due to very large extinction coefficient of InP at the corresponding photon energy (3.5 eV), most of the light will be reabsorbed by the material, generating free carriers that will contribute to band-edge luminescence. As the THG process has a cubic power dependence, the resulting light emission will adopt a similar power dependence. On the basis of bulk InP parameters the absorption length of 355 nm light is approximately 16 nm, so reabsorption will be a highly efficient process. Further measurements are needed to directly verify the presence of THG; however, the recent demonstration of efficient green light emission from THG in silicon microphotonic devices provides support for such a model.[20] We also note that Wang et al. has experimentally demonstrated an enhancement of the third-order nonlinearity in InP nanocrystals compared with bulk InP using *z*-scan measurements.[19,21]

By shifting the focus of the trapping laser with respect to the imaging system, we may probe different positions along the nanowire axis to observe the effects of changing the power density of the illuminating laser. This extends the range of incident intensities probed, while maintaining stable trapping conditions for the nanowire. In Figure 4d we observe power dependences of the emission for two different nanowires where the emission is collected from (i) a region at the trapping focus (diamonds) and (ii) a region away from the trapping focus (squares). In comparing these two graphs we observe that the power dependence changes from a cubic to a quadratic. This may be understood because as we move away from the trapping focus the beam diameter increases rapidly and the power density is reduced. These results suggest that both two and three photon related processes are taking place; i.e., direct absorption by two-photon absorption and third harmonic generation followed by reabsorption.

We may also consider other types of sum frequency generation processes where reabsorption is less pronounced; for example, second harmonic generation (SHG).[22] In this instance the higher energy photons should be directly observable. SHG has been observed in optically trapped $KNbO_3$ nanowires under continuous excitation by Nakayama et al.[23] and very recently in other perovskite alkaline nanowires in the work of Dutto et al.[24] SHG in nanowires has been demonstrated in a host of other semiconductor materials including ZnO,[25] GaN,[26] and ZnSe[27] where the materials have non-negligible bulk $\chi^{(2)}$ nonlinearity and are transparent in the spectral region of the incident and frequency doubled light. SHG in nanowires have characteristic properties of strong anisotropy due to depolarisation effects (in the electrostatic limit). InP also exhibits a $\chi^{(2)}$ nonlinear susceptibility, and the presence of hexagonal (WZ) phase regions, symmetry breaking points at the surface, and the presence of type-two heterostructures[28] may also contribute to the enhancement of SHG in these nanowires. Figure 5a displays the spectrum

dx.doi.org/10.1021/nl2020262 |*Nano Lett.* 2011, 11, 4149–4153

of SHG emission from a single optically trapped nanowire, as well as the nonlinear photoexcited photoluminescence from the same nanowire. The green SHG light emission is clearly visible to the naked eye, as is shown in the photograph in Figure 5b. Note that no green emission is observed when the trapping site is empty, confirming that the emission is from the optically trapped nanowire.

In conclusion we have investigated nonlinear photoexcitation processes in optically trapped InP nanowires. Our results indicate that a combination of two photon absorption and third harmonic generation followed by reabsorption are responsible for the corresponding band-edge emission. We observe significant differences in spectral features of the related are noted between nonlinear optical excitation and direct excitation and are related to the Burstein−Moss effect. Direct observation of second harmonic generation in trapped InP nanowires confirms the presence of nonlinear optical processes.

AUTHOR INFORMATION

Corresponding Author
*E-mail: p.reece@unsw.edu.au.

ACKNOWLEDGMENT

The authors thank the Australian Research Council for the financial support of this research. Australian National Fabrication Facility is acknowledged for the access to the nanowire growth facilities used in this work.

REFERENCES

(1) Cui, Y.; Lieber, C. M. *Science* **2001**, *291*, 851–853.
(2) Barrelet, C. J.; Greytak, A. B.; Lieber, C. M. *Nano Lett.* **2004**, *4*, 1981–1985.
(3) Skold, N.; Karlsson, L. S.; Larsson, M. W.; Pistol, M. E.; Seifert, W.; Tragardh, J.; Samuelson, L. *Nano Lett.* **2005**, *5*, 1943–1947.
(4) Pettersson, H.; Trägårdh, J.; Persson, A. I.; Landin, L.; Hessman, D.; Samuelson, L. *Nano Lett.* **2006**, *6*, 229–232.
(5) Yan, H.; Choe, H. S.; Nam, S.; Hu, Y.; Das, S.; Klemic, J. F.; Ellenbogen, J. C.; Lieber, C. M. *Nature* **2011**, *470*, 240–244.
(6) Duan, X. F.; Huang, Y.; Cui, Y.; Wang, J. F.; Lieber, C. M. *Nature* **2001**, *409*, 66–69.
(7) Mishra, A.; Titova, L. V.; Hoang, T. B.; Jackson, H. E.; Smith, L. M.; Yarrison-Rice, J. M.; Kim, Y.; Joyce, H. J.; Gao, Q.; Tan, H. H.; Jagadish, C. *Appl. Phys. Lett.* **2007**, *91*, 263104.
(8) Pemasiri, K.; Montazeri, M.; Gass, R.; Smith, L. M.; Jackson, H. E.; Yarrison-Rice, J.; Paiman, S.; Gao, Q.; Tan, H. H.; Jagadish, C.; Zhang, X.; Zou, J. *Nano Lett.* **2009**, *9*, 648–654.
(9) Wherrett, B. S. *J. Opt. Soc. Am. B* **1984**, *1*, 67–72.
(10) Reece, P. J.; Paiman, S.; Abdul-Nabi, O.; Gao, Q.; Gal, M.; Tan, H. H.; Jagadish, C. *Appl. Phys. Lett.* **2009**, *95*, 101109.
(11) Paiman, S.; Gao, Q.; Joyce, H. J.; Kim, Y.; Tan, H. H.; Jagadish, C.; Zhang, X.; Guo, Y.; Zou, J. *J. Phys. D: Appl. Phys.* **2010**, *43*, 445402.
(12) Pauzauskie, P. J.; Radenovic, A.; Trepagnier, E.; Shroff, H.; Yang, P.; Liphardt, J. *Nat. Mater.* **2006**, *5*, 97–101.
(13) Reece, P. J.; Toe, W. J.; Wang, F.; Paiman, S.; Gao, Q.; Tan, H. H.; Jagadish, C. *Nano Lett.* **2011**In Press.
(14) Nieminen, T. A.; Rubinsztein-Dunlop, H.; Heckenberg, N. R. *J. Quant. Spectrosc. Radiat. Transfer* **2003**, *79−80*, 1005–1017.
(15) Burstein, E. *Phys. Rev.* **1954**, *93*, 632–633.
(16) Kamat, P. V.; Dimitrijevic, N. M.; Nozik, A. J. *J. Phys. Chem.* **1989**, *93*, 2873–2875.
(17) Smith, L. M.; Jackson, H. E.; Yarrison-Rice, J. M.; Jagadish, C. *Semicond. Sci. Technol.* **2010**, *25*, 024010.
(18) Brandi, H. S.; de Araujos, C. B. *J. Phys. C: Solid State Phys.* **1983**, *16*, 5929.
(19) Hong-Li, W.; Dong, W.; Guang-De, C.; Hui, L. *Chin. Phys. Lett.* **2007**, *24*, 2600.
(20) Corcoran, B.; Monat, C.; Grillet, C.; Moss, D. J.; Eggleton, B. J.; White, T. P.; O'Faolain, L.; Krauss, T. F. *Nat. Photonics* **2009**, *3*, 206–210.
(21) Dvorak, M. D.; Justus, B. L. *Opt. Commun.* **1995**, *114*, 147–150.
(22) Cisek, R.; Barzda, V.; Ruda, H. E.; Shik, A. *IEEE J. Sel. Top. Quantum Electron.* **2010**, *PP*, 1–7.
(23) Nakayama, Y.; Pauzauskie, P. J.; Radenovic, A.; Onorato, R. M.; Saykally, R. J.; Liphardt, J.; Yang, P. *Nature* **2007**, *447*, 1098–1101.
(24) Dutto, F.; Raillon, C.; Schenk, K.; Radenovic, A. *Nano Lett.* **2011**, *11*, 2517–2521.
(25) Prasanth, R.; van Vugt, L. K.; Vanmaekelbergh, D. A. M.; Gerritsen, H. C. *Appl. Phys. Lett.* **2006**, *88*, 181501.
(26) Long, J. P.; Simpkins, B. S.; Rowenhorst, D. J.; Pehrsson, P. E. *Nano Lett.* **2007**, *7*, 831–836.
(27) Barzda, V.; Cisek, R.; Spencer, T. L.; Philipose, U.; Ruda, H. E.; Shik, A. *Appl. Phys. Lett.* **2008**, *92*, 113111.
(28) Bogani, F.; Cioncolini, S.; Lugagne-Delpon, E.; Roussignol, P.; Voisin, P.; André, J. P. *Phys. Rev. B* **1994**, *50*, 4554–4560.